Journal of Applied Polymer Science

Montmorillonite-Reinforced Sulfonated Poly(phthalazinone ether sulfone ketone) Nanocomposite Proton Exchange Membranes for Direct Methanol Fuel Cells

Zhengwen Hu,[1] Gaohong He,[1] Shuang Gu,[2] Yuanfa Liu,[1] Xuemei Wu[1]

[1]State Key Laboratory of Fine Chemicals, Research and Development Center of Membrane Science and Technology, School of Chemical Engineering, Dalian University of Technology, 2 Linggong Road, Dalian 116024, China

[2]Department of Chemical and Environmental Engineering, University of California-Riverside, 900 University Avenue, Riverside, California 92521

Correspondence to: G. He (E-mail: hgaohong@dlut.edu.cn)

ABSTRACT: To produce a composite membrane with high conductivity and low permeability, SPPESK with a degree of sulfonation of 101% was carefully selected for the preparation of montmorillonite (MMT)-reinforced SPPESK using solution intercalation. The fundamental characteristics such as water uptake, swelling ratio, proton conductivity, methanol permeability, and mechanical properties of the composite membranes were studied. Water uptake is improved when organic MMT (OMMT) loading increase. The composite membranes with CTAB-MMT loading of 4–0.5% show 0.143–0.150 S cm^{-1} proton conductivity at 80°C, which approaches the value of Nafion112. In addition, methanol permeability was decreased to 6.29×10^{-8} cm^2 s^{-1} by the addition of 6 wt % OMMT. As a result, the SPPESK-MMT composite membrane is a good candidate for use in direct methanol fuel cells. © 2013 Wiley Periodicals, Inc. J. Appl. Polym. Sci. **2014**, *131*, 39852.

KEYWORDS: clay; membranes; swelling; inorganic polymers; batteries and fuel cells

Received 12 March 2013; accepted 13 August 2013
DOI: 10.1002/app.39852

INTRODUCTION

Direct methanol fuel cells (DMFC) have attracted more and more attention in the past decade due to the high efficiency and low emission of pollutants. Perfluorosulfonic acid membranes, such as Dupont's Nafion membrane, have been widely used as proton exchange membranes in DMFCs.[1] However, the high permeability of the liquid methanol through Nafion membrane leads to reduced cathode voltage and cell performance. Therefore, it is highly desirable to find the low methanol permeability and high proton conductivity membrane.

To decrease methanol crossover, many researches have focused on alternative membranes based on the nonfluorinated polymer, for example, sulfonated poly(ether sulfones), sulfonated poly(ether ether ketone) (SPEEK), sulfonated poly(phthalazinone ether sulfone ketone) (SPPESK), sulfonated poly(2,6-dimethyl-1,4-phenylene oxide) (SPPO), sulfonated poly(arylene sulfone) (SPAS), sulfonated poly(phenylene sulfone).[2–10] These membranes show lower methanol permeabilities but also lower conductivities than Nafion. A general problem of homogeneous sulfonated arylene main-chain polymers is that these ionomers begin to swell too strong and thus lose their mechanical stability when a certain sulfonation degree (ion-exchange capacity 1.4–1.6 meq SO_3H/g) or a certain operation temperature (60–80°C) is exceeded. Therefore, it is required to reduce the swelling ratio of the membranes with high IEC.

Another feasible way to prepare composite membrane is by introducing some barrier of methanol permeation such as silicon oxide, titanium oxide and zirconium oxide, and montmorillonite (MMT) in polymer membrane.[11–15] Among the various inorganic, MMT is accepted as an excellent barrier for the permeation of small molecules.[16] For Nafion membrane, the high methanol permeability is the most disadvantages. MMT, HSO_3-MMT, Cloisite 10A, Cloisite 15A, Cloisite 30B, and Krytox-MMT were added into Nafion to decrease methanol crossover.[16–26] It was found that these MMTs not only decrease the methanol permeability, but also retain the high proton conductivity of membranes. LEE et al. reported that the different functionalized MMT (H-MMT, P-MMT, S-MMT, and F-MMT), when compared with commercial Nafion membranes, 50% of reduction in methanol permeability and the higher power density were achieved with inclusion of 5 wt % P-MMT in the composite membrane while proton conductivity

was reduced only by 12%.[27] Some researchers focused on the sulfonated aromatic polymer-MMT membrane such as, SPEEK-MMT, SPAS-MMT, and SPPO-MMT.[14,28–31] Their results show that the composite membranes with low MMT loading have good dimensionally stability, low methanol permeability, and high proton conductivity. M. M. Hasani-Sadrabadi reported that, after the optimum degree of sulfonation (DS), the S-PES nanocomposite membrane with 3.05% MMT content shows high conductivity, low methanol permeability, and excellent power density.[32]

Our previous researches show that SPPESK membrane has good thermal stability, mechanical property and proton conductivity.[6,33,34] It is believed that the SPPESK-MMT composite membrane should have higher performance, which is not reported, in this article, the organically modified MMT (OMMT) was prepared through ion exchange reaction between alkylammonium cations and metal cations. SPPESK was synthesized by sulfonating PPESK using the mixture of sulfuric acid and fuming sulfuric acid as sulfonating agent. The 101% of DS of SPPESK was carefully selected for the preparation of MMT-reinforced SPPESK using the solution intercalation. The microstructures of Na^+-MMT, OMMT, and SPEEK-MMT composite were compared. The fundamental characteristics such as water uptake, swelling ratio, proton conductive property, methanol permeability, and mechanical property of the composite membranes were studied.

MATERIALS AND METHODS

Materials

Na^+-MMT with cation exchange capacity of 0.98 mequiv g^{-1} was obtained from the Henan Nuclear Industry Hengda Factory. Cetyltrimethylammonium bromide (CTAB) was purchased from Tianjin Damao Chemical Reagents Factory. Sulfuric acid, fuming sulfuric acid, $AgNO_3$, and *N*-methylpyrrolidone (NMP) were provided by Tianjin Fuchen Chemical Reagents Factory. All used reagents are analytical grade.

Preparation of SPPESK

SPPESK was synthesized by sulfonating PPESK using the mixture of sulfuric acid (98 wt %) and fuming sulfuric acid (volume ratio of 4.6 : 5.4) as sulfonating agent. The detailed synthesis and separation method were reported in our previous work.[6] Finally, SPPESK with an IEC of 1.96 mmol g^{-1} and the sulfonation degree of 101% was carefully prepared.

Preparation of CTAB-Intercalated MMT (CTAB-MMT)

A mixture of Na^+-MMT in deionized water (0.03 g/mL) was stirred for 1 h, and then swelled for 24 h at room temperature to form dispersion. Subsequently, the CTAB solution was added dropwise in the dispersion under vigorous stirring. The resulting suspension was continuously stirred at 80°C for 6 h. After cooled to room temperature, the suspension was filtered and washed with deionized water to remove the superfluous surfactant until no bromide ion was detected by 0.1 mol/L $AgNO_3$ solution. The residual solid was dried at 80°C under vacuum for 24 h and then ground using an agate mortar. CTAB-MMT with particles size less than 50 μm were collected.

Preparation of MMT-Reinforced SPPESK (SPPESK-MMT) Membranes

Initially the certain amount of CTAB-MMT powder was ultrasonicated in NMP solvent for 2 h to form CTAB-MMT suspension, and then the suspension was vigorously mixed with the certain amount of SPPESK solution in NMP (10 wt %) at the given ratio of CTAB to SPPESK (0.5–6%). After additional ultrasonication for 2 h, the mixture was further stirred for 24 h at room temperature, and then the solution was casted on a clean glass plate and cured at 80°C for 12 h. Finally, the membrane was dried at 120°C for 12 h to remove the organic solvent. SPPESK-MMT membrane with thickness of about 70 μm was obtained.

Physical Characterization

A FT-IR spectrometer (BRUKER OPTICS, EQUINOX55) with the spectral resolution of 0.2 cm^{-1} was used to perform the IR characterization. The FR-IR spectra of Na^+-MMT and CTAB-MMT (in KBr pellets) were recorded in the wave number ranging from 500 to 4000 cm^{-1}. XRD measurements were carried out using a D/MAX-2400 with Cu Kα radiation. Diffraction data were collected at 0.20° s^{-1} steps between 1° and 10°.

Transmission electron microscopy (TEM) images were taken on a JEM-2000EX TEM at 120 Kv. The sample was embedded in plastic and thin section was cut by a glass knife using Ultra-microtome (LEICA EM UC6). Membrane stripes of 1×5 cm^2 were prepared for the mechanical property test. Tensile strength and tensile strain at break (elongation-to-break) of the membrane were measured by using a SANS CMT8102 stretching tester at the speed of 20 mm min^{-1}.

Water Uptake and Swelling Ratio

All membranes were immersed in deionized water for 24 h at room temperature. The membranes were wiped thoroughly before measuring the weight and dimension. The dry membranes were obtained from drying in vacuum for 24 h at 80°C. The water uptake and swelling ratio were calculated by the two following equations, respectively:

$$\text{Water uptake}(\%) = \frac{W_{wet} - W_{dry}}{W_{dry}} \times 100 \quad (1)$$

$$\text{Swelling ratio}(\%) = \frac{l_{wet} - l_{dry}}{l_{dry}} \times 100 \quad (2)$$

where W_{wet} and W_{dry} are the weight of wet and dry membrane sample, respectively; l_{wet} and l_{dry} are the average length [$l_{wet} = (l_{wet1} \times l_{wet2})^{1/2}$, $l_{dry} = (l_{dry1} \times l_{dry2})^{1/2}$] of wet and dry membrane sample, respectively.[34] l_{wet1}, l_{wet2}, l_{dry1}, and l_{dry2} are the lengths and widths of wet membranes and dry membranes, respectively.

Proton Conductivity

Prior to test, the membranes were soaked in 2*M* H_2SO_4 at room temperature for 48 h and then thoroughly washed and immersed in deionized water for 24 h. The proton conductivity was measured by a typical four-electrode AC impedance method using the Ivium A08001 impedance analyzer.[35] The frequency of

$1–10^5$ Hz was used for the impedance test. The proton conductivity was calculated from the following equation:

$$\sigma = \frac{L}{WdR} \quad (3)$$

where L is the distance between the two potential electrodes (1 cm), d and W are the thickness and width of the membrane sample, respectively, and R was derived from the right-side intersect of the semi-circle with the Re (Z) axis on the complex impedance plane.

Methanol Permeability

The methanol permeability of the membranes was determined using a home-made glass diffusion cell, which consists of two reservoirs (I and II) that are separated by a vertically placed membrane sample (effective area: 4.91 cm^2). Both reservoirs have the same volume of 20 mL. Reservoir I was filled with an aqueous solution of methanol (2M) and 1-butanol (40 g L^{-1}; used as an internal standard). Reservoir II was singularly filled with a 1-butanol (40 g L^{-1}) solution. The methanol concentration in reservoir II was measured using gas chromatography (FULI GC-9790II). Methanol concentration in the receiving cell detected as a function of time has the following relationship:

$$C_B(t) = \frac{A}{V_B}\frac{P}{L}C_A(t - t_0) \quad (4)$$

where, C_A and C_B are the methanol concentrations in reservoir I and II, respectively; V_B is the volume of reservoir II; A and L are the area and thickness of membrane samples, respectively; P is the methanol permeability; and t and t_0 are diffusion time and relaxation time, respectively.

RESULTS AND DISCUSSION

Preparation of SPPESK-MMT Nanocomposites

The first step is to prepare organically functionalized MMT to increase the gallery spacing through inserting large CTAB surfactant molecules. FTIR spectroscopy was used to confirm the organic functionalization. The IR spectra of the untreated MMT (Na^+-MMT) and the CTAB-treated MMT (CTAB-MMT) are shown in Figure 1. Before treatment, the Na^+-MMT spectrum shows strong IR absorptions at 400−600 cm^{-1} (Al—O stretching), 1038–1090 cm^{-1} (Si—O stretching), and around 3435 and 3628 cm^{-1} (O—H stretching in hydrogen-bond water and free water, respectively).[36] After CTAB treatment, the CTAB-MMT spectrum shows a pair of new peaks at 2851 and 2926 cm^{-1}, which are ascribed to the symmetrical and asymmetrical C—H stretching from CTAB molecules. In addition, the IR absorption of hydrogen-boned water (about 3435 cm^{-1}) apparently decreases in the CTAB-MMT spectrum, which can be explained by the direct interference from the CTAB molecule functionalization. Other characteristic absorptions in CTAB-MMT spectrum are similar to those in Na^+-MMT. Clearly, the comparison between untreated and treated IR spectra confirmed that the MMT had been successfully functionalized by CTAB.

The XRD analysis also provided further evidence for the CTAB functionalization. The XRD patterns of Na^+-MMT, CTAB-MMT, and SPPESK-MMT are shown in Figure 2. The MMT precursor, Na^+-MMT XRD pattern shows only one peak at 2θ of 6.96°, representing the original sheet spacing of 1.27 nm (n = 1). After CTAB functionalization, the CTAB-MMT shows one strong peak at 2θ of 2.31° and one moderate peak at 2θ of 4.62°, which represents the first order diffraction signal and the second one, respectively. Thus, the two peaks translate to 3.77 nm of d-spacing of the CTAB-modified MMT. The d-spacing is obviously larger for CTAB-MMT than for the original Na^+-MMT (3.77 vs. 1.27 nm), which clearly confirms that CTAB had been successfully intercalated into MMT.

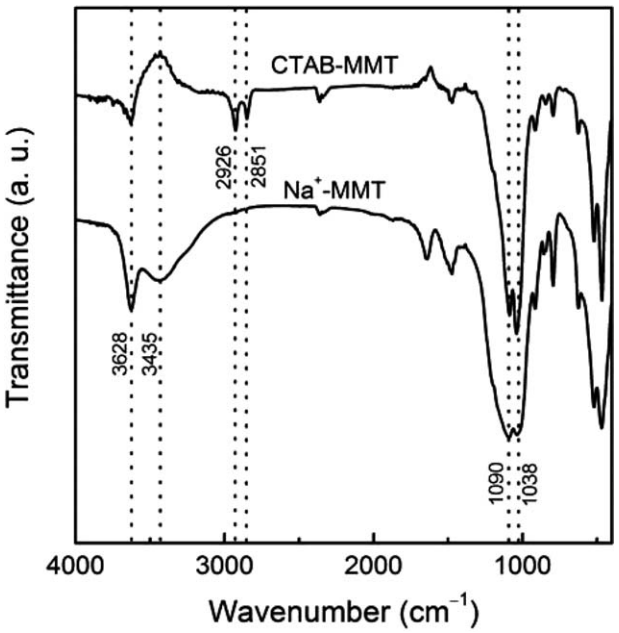

Figure 1. IR spectra of Na+−MMT and CTAB-MMT.

The MMT-reinforced SPPESK (SPPESK-MMT) composite membranes were prepared by the solution intercalation method.

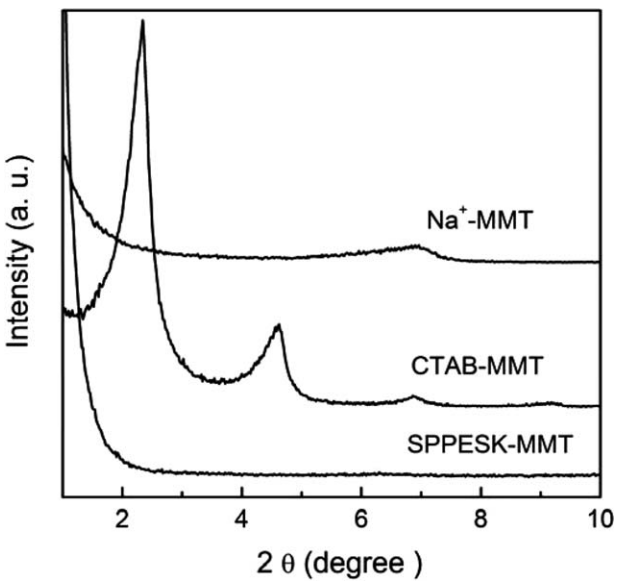

Figure 2. XRD patterns of Na+−MMT, CTAB-MMT, and SPPESK-MMT.

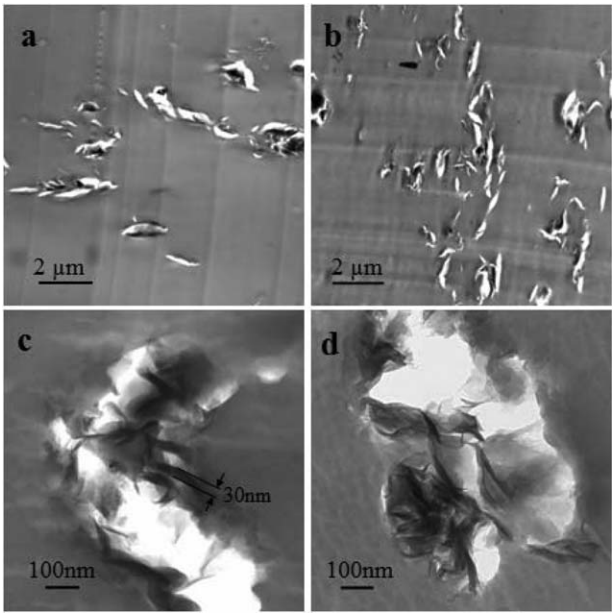

Figure 3. TEM images of SPPESK-MMT.

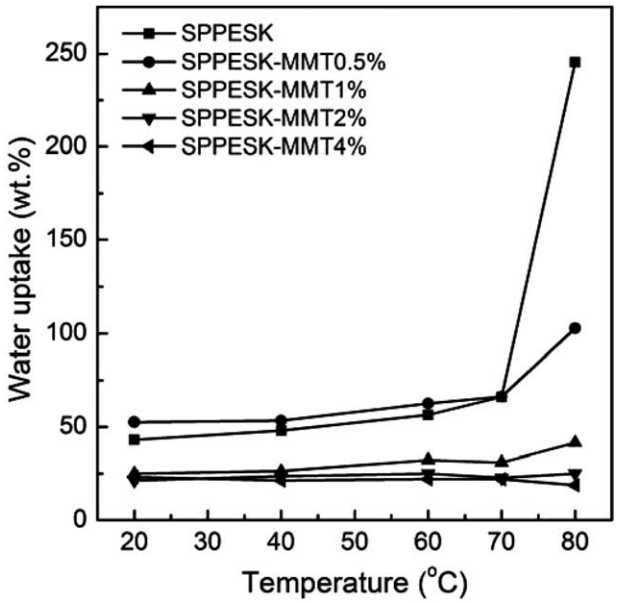

Figure 4. Water uptake of SPPESK-MMT membranes as function of water temperature.

As seen in Figure 2, the SPPESK-MMT composite shows no obvious peak within the test angle range (2θ: 1°–10°).

To investigate the dispersion of CTAB-MMT in SPPESK membrane, the TEM images of composite membrane are shown in Figure 3. The dark lines represent the MMT layers, the gray area denotes the SPPESK matrix, and the bright area is the damage due to glass knife during the sample preparation. Figure 3(a,b) show that the majority of CTAB-MMT still maintains the layered structure stacks and poorly distributes in SPPESK matrix. When the CTAB-MMT content is 1 wt % as shown in Figure 3(c), the size of agglomerated of MMT is about 30 × 100 × 100 nm^3, consisting of 5–10 layers. At the CTAB-MMT content of 4 wt %, more agglomerated MMT can be observed as shown in Figure 3(d). Although the CTAB-MMT is not completely exfoliated, the structural regularity becomes low, and some thin layers are observed. Thus, no obvious peak is observed by XRD in the tested angle range (2θ: 1°–10°).

Water Uptake and Swelling Ratio

The proton conductivity and methanol permeability of membrane are closely related to microstructure, such as cluster and channel size, which is influenced by the amount of water absorbed in the membrane[33]. Thus, the optimal water uptake is considered. Water uptake of pristine SPPESK membranes and SPPESK-MMT membranes are shown in Figure 4. The water uptake of pristine SPPESK membrane (DS: 101%) increases from 45 to 66% with temperature from 20 to 70°C and reaches as high as 230% at 80°C due to its very high IEC (1.96 mmol g^{-1}). Obviously, such a high water uptake restricts the pristine SPPESK membrane from being used in practical fuel cell applications, considering the typical working temperature of 80°C. As expected, the water uptake of composite membranes remarkably decreased with increasing CTAB-MMT loading at all test temperatures. Even with as low as 0.5% of CTAB-MMT loading, MMT reinforcement remarkably reduces the water uptake of SPPESK from 230% (SPPESK) to 80% (SPPESK-MMT0.5%) at 80°C, which suggests that MMT reinforcement is a very efficient and effective method. The higher CTAB-MMT loading leads to the much less water uptake: 4% of CTAB-MMT loading further reduced the water uptake to 26%, about one order of magnitude smaller than that of the original SPPESK (230%) at the same test temperature of 80°C.

The swelling ratios of SPPESK-MMT composite membranes with different CTAB-MMT loadings are shown in Figure 5. Similar to water uptake, the swelling ratio of SPPESK-MMT

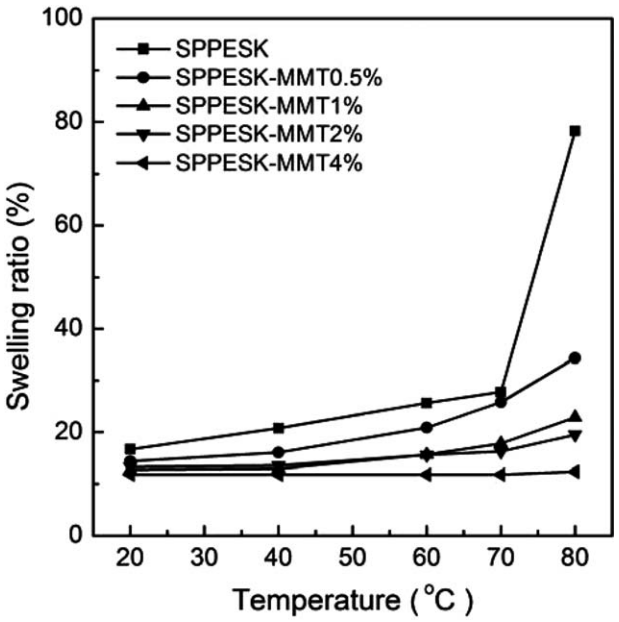

Figure 5. Swelling ratio of SPPESK-MMT membranes as function of temperature.

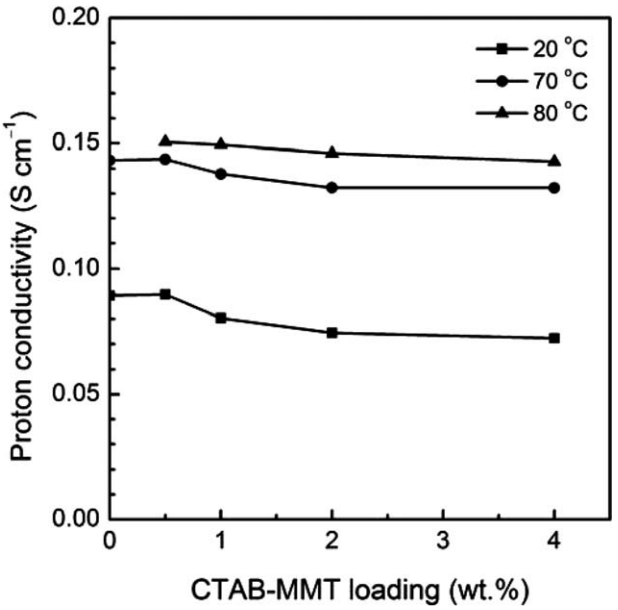

Figure 6. Proton conductivity of SPPESK-MMT membranes.

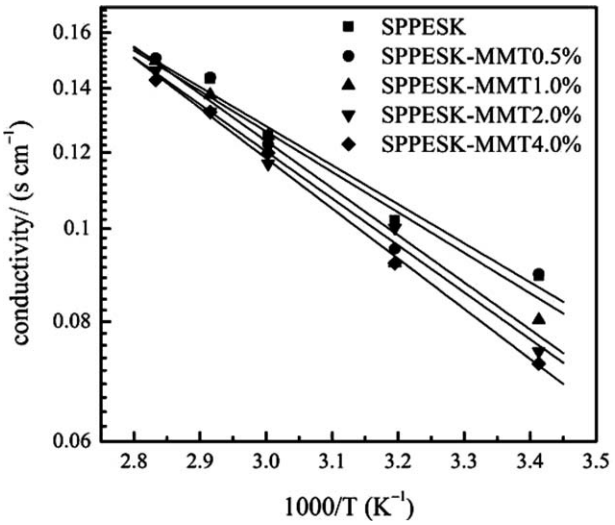

Figure 7. Conductivity of SPPESK and SPPESK-MMT depending on temperature.

composite membranes remarkably decreases with increasing the CATB-MMT loading at all test temperatures, clearly showing that the MMT-reinforcement has a very powerful and highly effective suppression against the membrane swelling. Obviously, the strong interaction between the well-dispersed nano-sheets of MMT and sulfonate groups of SPPESK strongly restricts the movement and relaxation of polymer chain, eventually reducing membrane swelling. Specifically, in comparison to the pristine SPPESK membrane swelling ratio (78%) at 80°C of test temperature, the swelling ratio of SPPESK-MMT composite membranes drastically lowers to 34, 23, 20, and 12% with the CTAB-MMT loading of 0.5, 1, 2, and 4%, respectively. These results clearly indicate that the SPPESK-MMT composite membranes have very good dimensional stability, and may be used directly in the DMFC application.

Proton Conductivity

The proton conductivity of SPPESK-MMT composite membranes with different CTAB-MMT loadings are shown in Figure 6. As expected, the conductivity slowly decreases with increasing the CTAB-MMT loading at all temperatures, because the well-dispersed MMT nano-sheets can more or less interfere with the proton transport through membranes. Taking test temperature at 20°C as an example, the proton conductivity moderately decreases from 0.090 to 0.070 S cm^{-1}, when the CTAB-MMT loading increases from zero to 4%. At 80°C, before the MMT reinforcement, the pristine SPPESK membrane swells too much and its proton conductivity cannot be measured. After the MMT reinforcement, the SPPESK-MMT composite membranes are dimensionally stable and thus their high proton conductivity is 0.143–0.150 S cm^{-1} with CTAB-MMT loading of 4–0.5%.

The proton conductivity dependence on temperature of SPPESK-MMT composite membranes are shown in Figure 7. According to the Arrhenius relationship, the activation energy of proton conductivities is calculated and the results are listed in Table I. Apparently, the activation energy slightly increases from 7.8 to 10.1 kJ mol^{-1} with increasing the CTAB-MMT loading from zero to 4%. This suggests that the interference of the MMT with proton conduction will be favorably alleviated at elevated temperatures. Practically, the MMT may have very limited, or even negligible, impact on the proton conductivity of SPPESK-MMT composite membranes, considering the high working temperature is more frequently used in fuel cell operations.

Methanol Permeability

Methanol crossover through PEMs leads to fuel waster and more severely cell voltage drop in DMFC applications. Thus reducing the methanol permeability has been one of the major challenges in developing high-performance PEMs. The methanol permeabilities of pristine SPPESK and SPPESK-MMT membranes at 25°C are presented in Figure 8. The SPPESK membrane has a methanol permeability of 1.28 × 10^{-7} cm^2 s^{-1}, which is very close to those of SPPESKs (around 1 × 10^{-7} cm^2 s^{-1}) reported in our previous work[6]. The slightly higher number we measured here is most likely due to the higher test temperature we used here (25 vs. 15°C). Clearly, methanol permeability decreases continuously from 1.28 × 10^{-7} to 6.29 × 10^{-8} cm^2 s^{-1} with increasing CTAB-MMT loading from zero to 6%. More than half of reduction of methanol permeability clearly indicates that MMT serves as an excellent methanol barrier indeed. It is believed that well-dispersed MMT nano-sheets

Table I. Activation Energy of SPPESK-MMT Membranes

Membrane	Ea (kJ mol^{-1})
SPPESK	7.8 ± 1.0
SPPESK-MMT0.5%	8.1 ± 1.3
SPPESK-MMT1%	9.4 ± 0.9
SPPESK-MMT2%	9.4 ± 0.5
SPPESK-MMT4%	10.0 ± 0.3

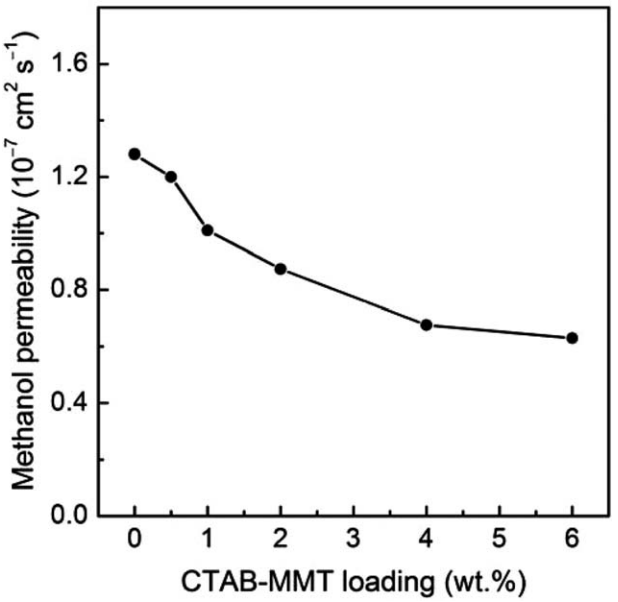

Figure 8. Methanol permeability of pristine SPPESK and SPPESK-MMT membranes.

(typically about 1 nm of thickness and around 100 nm of length) can drastically block the diffusion pathways of methanol, eventually reducing methanol permeability considerably.

Membrane Selectivity

Both methanol permeability and proton conductivity are the important factors, and in most cases they increase or decrease at the same direction. Thus, the membrane selectivity (defined as the ratio of proton conductivity to methanol permeability) is very helpful to illustrate their over-all balance. Figure 9 shows the membrane selectivity of composite membranes with different MMT loading, and the membrane selectivity apparently

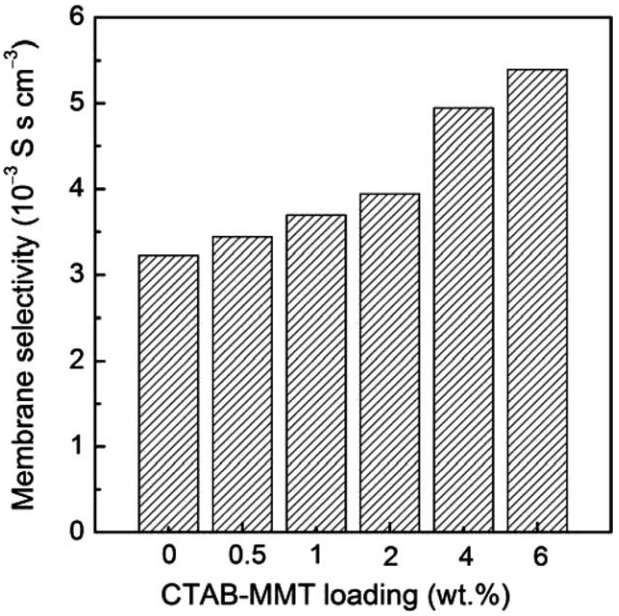

Figure 9. Membrane selectivity of SPPESK-MMT with at different CTAB-MMT loadings.

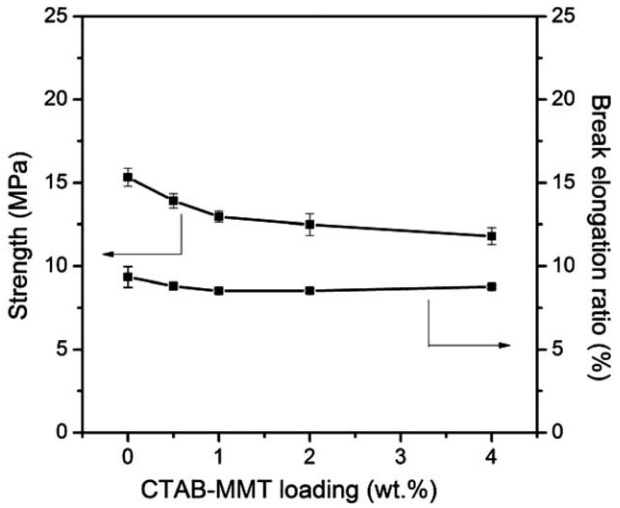

Figure 10. Tensile strength and elongation-to-break of SPPESK-MMT composite membranes.

with increasing MMT loading. Although both proton conductivity and methanol permeability decrease with increasing CTAB-MMT loading, the methanol permeability decreases in a more rapid way than the proton conductivity does.

Mechanical Property

The tensile strength and elongation-to-break of SPPESK-MMT composite membranes with different CTAB-MMT loadings are shown in Figure 10. Whether or not the CTAB-MMT was added, the elongation-to-break remains almost unchanged at a level of about 9%, indicating that the addition of MMT does not affect the membrane flexibility. On the other hand, the tensile strength of composite membranes slightly decreases from 15.3 MPa to 11.8 MPa (or to about 80%) with increasing CTAB-MMT loading from zero to 4%. The possible reason is that the MMT may not perfectly dispersed thorough SPPESK, but aggregate together to some extent in some region that directly leads to the material failure. Since well-dispersed MMT had been found to slightly improve the tensile strength of membrane, it is believed that the SPPESK-MMT composite membranes may do even better if MMT dispersion can be improved in the future work.[22,37]

CONCLUSION

SPPESK-MMT composite membranes were prepared by the solution intercalation methods. The fundamental characteristics such as water uptake, swelling ratio, proton conductive property, methanol permeability, and mechanical property of the composite membranes were investigated. The water uptake and swelling ratio of composite membranes remarkably decreased with increasing CTAB-MMT loading at all test temperatures. After the MMT reinforcement, the SPPESK-MMT composite membranes are dimensionally stable and thus the high proton conductivity is 0.143–0.150 S cm^{-1} with CTAB-MMT loading of 4–0.5%. Methanol permeability decreases continuously from 1.28×10^{-7} to 6.29×10^{-8} cm^2 s^{-1} with increasing CTAB-MMT loading from zero to 6%. These results indicate that the

SPPESK-MMT composite membrane offers promise for use in DMFCs.

ACKNOWLEDGMENTS

The authors thank the support of National Science Fund for Distinguished Young Scholars of China (Grant no.21125628) and National Natural Science Foundation of China (Grant no. 21176044).

REFERENCES

1. Kerres, J. A. *J. Membr. Sci.* **2001**, *185*, 3.
2. Li, L.; Xu, L.; Wang, Y. X. *Acta Polym. Sci.* **2003**, *465*, 4.
3. Kreuer, K. D. *J. Membr. Sci.* **2001**, *185*, 29.
4. Xue, Y. H.; Fu, R. Q.; Wu, C. M.; Lee, J. Y.; Xu, T. W. *J. Membr. Sci.* **2010**, *350*, 148.
5. Du, L.; Yan, X. M.; He, G. H.; Wu, X. M.; Hu, Z. W.; Wang, Y. D. *Int. J. Hydrogen Energy* **2012**, *37*, 11853.
6. Gu, S.; He, G. H.; Wu, X. M.; Li, C. N.; Liu, H. J.; Lin, C.; Li, X. C. *J. Membr. Sci.* **2006**, *281*, 121.
7. Haghighi, A. H.; Hasani-Sadrabadi, M. M.; Dashtimoghadam, E.; Bahlakeh, G.; Shakeri, S. E.; Majedi, F. S.; Emami, S. H.; Moaddel, H. *Int. J. Hydrogen Energy* **2011**, *36*, 3688.
8. Yun, S. H.; Woo, J. J.; Seo, S. J.; Wu, L. A.; Wu, D.; Xu, T. W.; Moon, S. H. *J. Membr. Sci.* **2011**, *367*, 296.
9. Joo, S. H.; Pak, C.; Kim, E. A.; Lee, Y. H.; Chang, H.; Seung, D.; Choi, Y. S.; Park, J. B.; Kim, T. K. *J. Power Sources* **2008**, *180*, 63.
10. Saarinen, V.; Kreuer, K. D.; Schuster, M.; Merkle, R.; Maier, J. *Solid State Ionics* **2007**, *178*, 533.
11. Mahreni, A.; Mohamad, A. B.; Kadhum, A. A. H.; Daud, W. R. W.; Iyuke, S. E. *J. Membr. Sci.* **2009**, *327*, 32.
12. Profeti, L. P. R.; Profeti, D.; Olivi, P. *Int. J. Hydrogen Energy* **2009**, *34*, 2747.
13. Silva, V.; Ruffmann, B.; Silva, H.; Mendes, A.; Madeira, M.; Nunes, S. *Adv. Mater. Forum Ii* **2004**, *455-456*, 587.
14. Chang, J. H.; Park, J. H.; Park, G. G.; Kim, C. S.; Park, O. O. *J. Power Sources* **2003**, *124*, 18.
15. Xing, D. M.; He, G. H.; Hou, Z. J.; Ming, P. W.; Song, S. F. *Int. J. Hydrogen Energy* **2011**, *36*, 2177.
16. Song, M. K.; Park, S. B.; Kim, Y. T.; Kim, K. H.; Min, S. K.; Rhee, H. W. *Electrochim. Acta* **2004**, *50*, 639.
17. Jung, D. H.; Cho, S. Y.; Peck, D. H.; Shin, D. R.; Kim, J. S. *J. Power Sources* **2003**, *118*, 205.
18. Silva, R. F.; Passerini, S.; Pozio, A. *Electrochim. Acta* **2005**, *50*, 2639.
19. Rhee, C. H.; Kim, H. K.; Chang, H.; Lee, J. S. *Chem. Mater.* **2005**, *17*, 1691.
20. Kim, Y.; Lee, J. S.; Rhee, C. H.; Kim, H. K.; Chang, H. *J. Power Sources* **2006**, *162*, 180.
21. Lin, Y. F.; Yen, C. Y.; Hung, C. H.; Hsiao, Y. H.; Ma, C. C. M. *J. Power Sources* **2007**, *168*, 162.
22. Kim, T. K.; Kang, M.; Choi, Y. S.; Kim, H. K.; Lee, W.; Chang, H.; Seung, D. *J. Power Sources* **2007**, *165*, 1.
23. Song, M. K.; Kim, Y. M.; Kim, Y. T.; Rhee, H. W.; Smirnova, A.; Sammes, N. M.; Fenton, J. M. *J. Electrochem. Soc.* **2006**, *153*, A2239.
24. Jaafar, J.; Ismail, A. F.; Matsuura, T. J. *Appl. Polym. Sci.* **2012**, *124*, 969.
25. Thomassin, J. M.; Pagnoulle, C.; Caldarella, G.; Germain, A.; Jerome, R. *Polymer* **2005**, *46*, 11389.
26. Gosalawit, R.; Chirachanchai, S.; Shishatskiy, S.; Nunes, S. P. *Solid State Ionics* **2007**, *178*, 1627.
27. Lee, W.; Kim, H.; Kim, T. K.; Chang, H. *J. Membr. Sci.* **2007**, *292*, 29.
28. Gosalawit, R.; Figoli, A.; Chirachanchai, S. *Asia-Pac. J. Chem. Eng.* **2010**, *5*, 60.
29. Choi, Y. S.; Kim, T. K.; Kim, E. A.; Joo, S. H.; Pak, C.; Lee, Y. H.; Chang, H.; Seung, D. *Adv. Mater.* **2008**, *20*, 2341.
30. Kim, D. J.; Hwang, H. Y.; Nam, S. Y.; Hong, Y. T. *Macromol. Res.* **2012**, *20*, 21.
31. Hasani-Sadrabadi, M. M.; Emami, S. H.; Moaddel, H. *J. Power Sources* **2008**, *183*, 551.
32. Hasani-Sadrabadi, M. M.; Dashtimoghadam, E.; Ghaffarian, S. R.; Sadrabadi, M. H. H.; Heidari, M.; Moaddel, H. *Renew. Energy* **2010**, *35*, 226.
33. Wu, X. M.; He, G. H.; Gu, S.; Hu, Z. W.; Yan, X. M. *Chem. Eng. J.* **2010**, *156*, 578.
34. Gu, S.; He, G. H.; Wu, X. M.; Guo, Y. J.; Liu, H. J.; Peng, L.; Xiao, G. K. *J. Membr. Sci.* **2008**, *312*, 48.
35. Gu, S.; Cai, R.; Luo, T.; Chen, Z. W.; Sun, M. W.; Liu, Y.; He, G. H.; Yan, Y. S. *Angew. Chem. Int. Ed.* **2009**, *48*, 6499.
36. Praus, P.; Turicova, M.; Studentova, S.; Ritz, M. *J. Colloid Interface Sci.* **2006**, *304*, 29.
37. Gosalawit, R.; Chirachanchai, S.; Shishatskiy, S.; Nunes, S. P. *J. Membr. Sci.* **2008**, *323*, 337.